Title

CALCULATED THERMODYNAMIC DATA ANDMETASTABLE IMMISCIBILITY IN THE SiO -Al 0 SYSTEM

Author

Risbud, Subhash H.

Publication Date

1976-10-01

Submitted to American Ceramic Society

LBL-4190
Preprint

CALCULATED THERMODYNAMIC DATA AND METASTABLE IMMISCIBILITY IN THE SiO_2-Al_2O_3 SYSTEM

Subhash H. Risbud and Joseph A. Pask

October 1976

Prepared for the U. S. Energy Research and
Development Administration under Contract W-7405-ENG-48

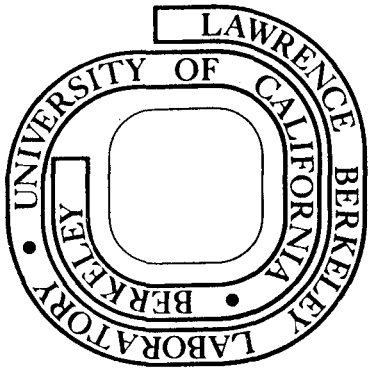

DISCLAIMER

CALCULATED THERMODYNAMIC DATA AND METASTABLE IMMISCIBILITY IN THE SiO_2-Al_2O_3 SYSTEM

Subhash H. Risbud* and Joseph A. Pask

Materials and Molecular Research Division, Lawrence Berkeley Laboratory
and Department of Materials Science and Engineering,
University of California, Berkeley, California 94720

ABSTRACT

Thermodynamic data on activities, activity coefficients and free energies of mixing in SiO_2-Al_2O_3 solutions was obtained from the phase diagram using regular solution approximations. The marked positive deviations from ideal mixing in the thermodynamic data suggest a tendency for liquid immiscibility in both SiO_2 and Al_2O_3-rich compositions. The calculated data were used to estimate regions of liquid-liquid immiscibility. A metastable liquid miscibility gap with a consolute temperature of ≈1540°C at a critical composition of ≈36 mole% Al_2O_3 was calculated; the gap extended from ≈7 to 57 mole% Al_2O_3 at a temperature of ≈800°C. SiO_2-rich glass compositions were prepared and examined for liquid phase separation by direct transmission electron microscopy.

* Now an Assistant Professor in the Mechanical Engineering Department, University of Nebraska.

I. INTRODUCTION

The important role of initial liquid phase separation in glass processing and crystallization is well known.[1] Assessment of regions of liquid immiscibility on the phase diagram is, therefore, of considerable value especially in well known glass forming systems. The question of metastability and possible immiscibility in the SiO_2-Al_2O_3 binary system has been raised by several investigations.

Galakhov and Konovalova[2] reported petrographic observations on binary SiO_2-Al_2O_3 mixtures ranging in composition from 20 to 60 wt% (13 to 46 mol%) Al_2O_3 as a basis for suggesting "micro" and "macro" immiscibility. Ganguli and Saha[3] studied SiO_2-Al_2O_3 glasses in the range 6 to 21 wt% (3.5 to 13 mol %) Al_2O_3 and found no evidence for an immiscibility dome although their observations represented non-equilibrium conditions. MacDowell and Beall[4] conducted an extensive study of SiO_2-Al_2O_3 glasses in the composition range 0-72 wt% (0-60 mol %) Al_2O_3. Examination of the morphology of quenched glass-crystalline mixtures by electron microscopy indicated a strong tendency for phase separation in the composition range ≈10 to 68 wt%(≈7 to 55 mol %) Al_2O_3 at 1100°C. The range of temperatures at which this phase separation occurred was not clear from the reported data but a miscibility gap was proposed with an upper consolute temperature of ~1650°C at a critical composition between ~38 to 42 wt% (~25 to 30 mol %) Al_2O_3. Takamori and Roy[5] considered the evidence in favor of the proposed miscibility gap to be inadequate in light of their DTA and TEM observations on splat cooled SiO_2-Al_2O_3 glasses in the composition range (≈20 to 95 mol %) Al_2O_3. No evidence for the location of the miscibility gap could be

found in their data.

The experimental difficulties in delineating immiscibility regions in the present system are understandable in view of the problems associated with rapid quenching of melts from high temperatures (~2000°C) and also because of the tendency of compositions greater than ~30 mol % Al_2O_3 to crystallize readily.[4] Mindful of the experimental problems, an approach utilizing calculations from the stable phase diagram has been used in the present study to calculate departures from ideal solution behavior. These enable an estimation of the approximate composition ranges where immiscibility can be expected to occur in the SiO_2-Al_2O_3 binary system.

II. ANALYSIS PROCEDURES AND SOLUTION THERMODYNAMICS

Adequate descriptions of the thermodynamics of silicate melts require data on the species present and their interactions during solution mixing. Models based on the regular solution approximation have been used to calculate thermodynamic data in metal-slag systems,[6] fused salts,[7] and silicates.[8] Adopting a similar approach, Charles described procedures for calculation of activities in alkali-silicates[9] and B_2O_3-SiO_2 solutions[10] and obtained an estimate of the miscibility gaps in these systems. The procedures entail the use of the heat of fusion, which is assumed to stay constant with temperature, and the position of

the liquidus curve on the phase diagram to obtain the activity of the component through the equation:

$$\log_{10} a^L = \frac{\Delta H_m}{4.575} \left[\frac{1}{T_m} - \frac{1}{T_L}\right] = \log_{10} a^S \qquad (1)$$

where a^L = activity of the liquid in the liquidus composition referred to pure liquid standard state.

a^S = activity of solid at the liquidus temperature referred to pure liquid standard state.

ΔH_m = heat of melting, cal/mol.

T_m = melting temperature, °K.

T_L = liquidus temperature, °K.

The data calculated along the liquidus can then be extrapolated to other temperatures by assuming that at a fixed composition the partial heat of solution, ΔH, stays independent of temperature.[9] Thus,

$$RT_L \log_{10} \gamma_L = RT \log_{10} \gamma_T \qquad (2)$$

where T_L and γ_L = liquidus temperature and activity coefficient at the liquidus, respectively

T and γ_T = temperature and activity coefficient at the chosen temperature T.

R = gas constant = 1.98 cal/mol°K.

The calculated isothermal activity coefficients for one component can then be used in the Gibbs-Duhem equation to obtain data for the other component in the binary system:

$$X_1 \, d \log \gamma_1 + X_2 \, d \log \gamma_2 = 0 \qquad (3)$$

where X_1 and X_2 = mole fractions of components 1 and 2.

γ_1 and γ_2 = activity coefficients of components 1 and 2, respectively.

The calculated activities can now be assembled in the following

equation to obtain the free energy of mixing of the liquids, ΔG_m, at a temperature T

$$\Delta G_m = RT \quad X_1 \ell n\ a_1 + X_2\ \ell n\ a_2 \tag{4}$$

where a_1 and a_2 = activities of component 1 and 2.
The variation of the free energy of mixing with composition can be used to locate the width of the miscibility gap at each temperature.

Application of the above procedures to the SiO_2-Al_2O_3 binary system require a well-considered choice of mixing species participating in the regular solution process. For the alkali silicates and borates, Haller et al.[11] proposed the use of a SiO_2 or B_2O_3 multimer and the stoichiometric compound limiting the miscibility gap at the alkali end as the two immiscible liquids. SiO_2 or B_2O_3 multimers were chosen to satisfy the shape of experimentally reported gaps in these systems. In the absence of any structural data on the species present in SiO_2-Al_2O_3 melts various stable and metastable binary phase relationships proposed by Aksay and Pask[12] (Fig. 1), were considered in choosing species for the mixing process. For instance, if the metastable SiO_2-3:2 mullite (58.0 mole% Al_2O_3) binary system is considered, the liquid phase separation process could be visualized in terms of the following reaction:

$$xSiO_2 \cdot yAl_2O_3(\ell) \rightleftharpoons XSiO_2(\ell) + Y\left[Al_{1.16}\ Si_{0.42}\ O_{2.58}(\ell)\right] \tag{5}$$

where x and y are the mole fractions of SiO_2 and Al_2O_3 in the starting composition and X and Y are the mole fractions of the unmixed liquids. Similarly, if the metastable SiO_2-2:1 mullite (66.7 mole% Al_2O_3) system is considered, the phase separation reaction can be

written as:

$$xSiO_2 \cdot yAl_2O_3(\ell) \rightleftharpoons X\ SiO_2(\ell) + Y\left[Al_{1.34}\ Si_{0.33}\ O_{2.67}\ (\ell)\right] \quad (6)$$

III. RESULTS AND DISCUSSION

A. Calculated Thermodynamic Data

1. SiO_2 Liquidus

The cryoscopic data obtained from the SiO_2 liquidus (Fig. 1), assuming the mixing species to follow reaction (5) above, is listed in Table 1. This data was calculated from Eqs. 1 and 2 using a heat of fusion of 1835 cal/mole[13] and a melting point of 1986°K[13] for SiO_2. The very small positive deviations from ideal mixing shown in Table 1 suggests that immiscibility in the composition range spanned by the SiO_2 liquidus (0 to ~5 mole % Al_2O_3) may not occur sufficiently above glass transition temperatures (~1100°C for SiO_2).

2. Mullite Liquidus

Activities along the mullite liquidus curve of the metastable SiO_2-3:2 mullite (58.0 mole % Al_2O_3) system using the mullite compositions in equilibrium with liquid, can be obtained from Eq. 1. However, no experimentally reported value for the heat of fusion of mullite was available. A value can be obtained by two approaches.

A value can be calculated if isothermal activities are known. Since a correspondence must exist for SiO_2 activities at a fixed composition and temperature the isothermal activities of SiO_2 obtained in the composition range spanned by the mullite liquidus (using Eqs. 1 to 3) can be matched with the activities obtained from the SiO_2 liquidus when extended metastably to higher mullite mole fractions. This approach yields a value for the heat of fusion of mullite of ~27,000 cal/mole.

The second approach consists of estimating the heat of fusion on the basis of weighted averages of the heats of fusion of the constituents

Al_2O_3 and SiO_2. Using the experimentally reported heats of fusion of Al_2O_3 and SiO_2 of 25,700 cal/mole[14] and ~1835 cal/mole,[13] respectively, the heat of fusion of mullite (0.58 Al_2O_3 0.42 SiO_2) can be estimated to be

$$0.58(25,700) + 0.42\ (1835) \simeq 16,000 \text{ cal/mole.}$$

In view of the lack of a measured value of the heat of fusion of mullite and because calculated activities (Eq. 1) are greatly dependent on the value chosen, data were calculated for a range of values of the heat of fusion from 16,000 to 54,000 cal/mole in order to determine the sensitivity to this value. The critical points for immiscibility were estimated for each set of data. Similar considerations were used in the analysis of the metastable SiO_2-2:1 mullite (0.67 Al_2O_3 0.33 SiO_2), and SiO_2-2:1 mullite (0.75 Al_2O_3 0.25 SiO_2) systems.

A representative set of thermodynamic data for the metastable SiO_2-3:2 mullite (0.58 $Al_2O_3 \cdot 0.42\ SiO_2$) system using the calculated heat of fusion for mullite of 27,000 cal/mole is shown in Table II which lists the cryoscopic data from the mullite liquidus metastably extended to ~58 mole % Al_2O_3. Isothermal data at chosen subliquidus temperatures can then be obtained based on the previously stated assumptions regarding the constancy of the partial molal heat of solution[9] (Eq. 2). This type of assumption has been reported to show good agreement with calorimetric results for the PbO-SiO_2 system in the temperature range 900°-1700°C.[15] As shown in Fig. 2 the activity coefficients of mullite indicate a strong positive deviation from ideal mixing. The data of Fig. 2 can then be used in Eq. 3 to obtain isothermal data for SiO_2 (ℓ) (Fig. 3); considerable non-ideality is also apparent from these data.

Similar behavior is indicated by selection of other mullite species and heats of fusion.

3. Al_2O_3 Liquidus

The Al_2O_3 liquidus curve (Fig. 1) was analyzed in the composition range 40 to 100 mole % Al_2O_3. The activities of Al_2O_3 were calculated from Eq. 1 using experimentally reported values of the heat of fusion 25,700 cal/mole[14] and melting temperature[14] (2323°K) of Al_2O_3. In order to obtain the data on activity coefficients for the reacting components a choice of the species involved in the solution mixing is necessary. Since no information on the exact nature of the mixing species is available to warrant a specific choice, two possibilities were considered.

On the one extreme SiO_2 and Al_2O_3 can be selected as the end components of the pseudobinary system; and on the other, mullite ($\sim 0.6Al_2O_3 \cdot 0.4SiO_2$) and Al_2O_3 could be considered as the components. Activity coefficients and partial molal heats of solution of Al_2O_3 in these two cases are listed in Tables III and IV, respectively. The positive values of $\log_{10}\gamma_{Al_2O_3}$ and the partial molal heats of solution of Al_2O_3 indicate a strong positive departure from an ideal solution. Isothermal data for $\log_{10}\gamma_{Al_2O_3}$ using SiO_2 and Al_2O_3 as the components is presented in Fig. 4. The activities of Al_2O_3 at several subliquidus temperatures are shown in Fig. 5. Imminent unmixing is indicated below ~1100°C. The data of Fig. 4 can also be used in Eq. (3) to obtain isothermal values of $\log_{10}\gamma_{SiO_2}$ (Fig. 6). The activity coefficients of SiO_2, Al_2O_3 and mullite obtained above are such that the integral molal heat of mixing $\Delta H^M = (X_1 \overline{\Delta H}_1 + X_2 \overline{\Delta H}_2)$ has a positive value. A marked

tendency toward liquid immiscibility is therefore implied in these data.

4. "Regular" Behavior of SiO_2-Al_2O_3 Solutions

The parabolic nature of the variation of the isothermal activity coefficients of SiO_2 (logarithmic) as shown in Figs. 3 and 6 suggests that SiO_2-Al_2O_3 solutions may behave in a "regular" manner. Such behavior may be tested by plotting the α-function suggested by Hildebrand and Scott;[16] the constancy of α with composition indicates a regular solution with a constant heat of mixing and ideal entropy of mixing. For equal molar volumes, the α- function in the present system can be defined as:

$$\alpha = \frac{\log_{10}\gamma_{SiO_2}}{\left(X_{Al_2O_3}\right)^2} = \frac{\log_{10}\gamma_{Al_2O_3}}{\left(X_{SiO_2}\right)^2} \qquad (7)$$

Isothermal values of $\log_{10}\gamma_{SiO_2}$ are shown in Fig. 6 in the composition range 40 to 100 mole % Al_2O_3 (assuming SiO_2 and Al_2O_3 as components). The $\log_{10}\gamma_{SiO_2}$ data in Fig. 3 was obtained by treating SiO_2 and mullite as components in the composition range 0 to 100 mole % mullite (i.e. 0 to ~58 mole % Al_2O_3). Since the activity of SiO_2 in the solution at a fixed composition must be the same regardless of the components chosen, the $\log_{10}\gamma_{SiO_2}$ data of Fig. 3 can be converted to a new set of $\log_{10}\gamma_{SiO_2}$ values referred to SiO_2 and Al_2O_3 as components. Thus

$$\log_{10}\gamma^{M}_{SiO_2} + \log_{10}X^{M}_{SiO_2} = \log_{10}\gamma^{A}_{SiO_2} + \log_{10}X^{A}_{SiO_2},$$

i.e. log(Activity of SiO_2) = log(Activity of SiO_2),

where $\gamma^{M}_{SiO_2}$, $X^{M}_{SiO_2}$ and $\gamma^{M}_{SiO_2}$, $X^{M}_{SiO_2}$ are activity coefficients and mole fractions of SiO_2 with mullite and Al_2O_3 as components, respectively. The α values for each temperature can now be calculated from Eq. (7).

As shown in Fig. 7 α stays essentially constant in the composition range ~15 to 95 mole % Al_2O_3. The reasonable approximation to regular behavior indicated in this data thus support the approach used in the present study to calculate the thermodynamic data from the phase diagram.

B. Metastable Liquid-Liquid Immiscibility

The thermodynamic data obtained in the previous section were assembled in the expression $\Delta G_m = RT [X_1 \ln a_1 + X_2 \ln a_2]$ (Eq. 4), to obtain the isothermal free energy of mixing values referred to pure liquid standard states. The variation of the free energy of mixing with composition was then used to locate the width of the miscibility gap at each temperature.

1. Immiscibility in the SiO_2 - Mullite System

The data shown in Figs. 2 and 3 was assembled to obtain the isothermal free energy of mixing values for the metastable SiO_2-3:2 mullite (0.58 Al_2O_3 0.42 SiO_2) system using a value of ΔH_f = 27,000 cal/mole. Common tangents to the resulting plot of ΔG_m vs. composition (Fig. 8) represent the compositions at the boundary of the miscibility gap at each temperature shown in Fig. 1;its indicated spinodal is also based on data provided by Fig. 8.

As stated previously, the calculated thermodynamic data are dependent on the value of the heat of fusion of mullite and the end components chosen in the mixing model. Consequently, the effect of the heat of fusion value on the calculated immiscibility was evaluated for a range of values of mullite heat of fusion (Table V). As shown in the table the upper consolute temperature of the miscibility gap is significantly lowered with an increasing value for the heat of fusion. The critical

composition is, however, not significantly affected. Figure 1 also shows the calculated miscibility gap using the value of 16,000 cals/mole for the heat of fusion of mullite. The calculated miscibility gap shown for SiO_2-2:1 mullite (0.67 Al_2O_3 0.33 SiO_2) as components used an estimated heat of fusion of 18,000 cal/mole for 2:1 mullite. The upper consolute temperature of the miscibility gap is raised when a higher Al_2O_3 mullite is chosen as a component in the calculation. The shape of the miscibility gap is thus sensitive to the composition of heat of fusion values used for the mullite species.

It would be expected that the miscibility gap derived by using SiO_2 and 3:2 mullite (0.58 mole % Al_2O_3) as components and the heat of fusion of 27,000 cal/mole calculated from the phase diagram would be the most likely to be accurate. This conclusion is supported by the fact that the extended Al_2O_3 liquidus does not intersect the miscibility gap (See Fig. 1) which is thermodynamically required. The gap has a consolute temperature of ≈1540°C, a width from ~11 to ~49 mole % Al_2O_3 at 1100°C, and intersects the curve for glass transformation temperatures ($\eta \approx 10^{14.6}$ poises) estimated from viscosity data[17] at ~7 (at~800°C) and ~56 (at~600° C) mole % Al_2O_3. This curve represents the lower limit for experimentally realizable immiscibility. The corresponding values for the gap calculated by using a heat of fusion value of 16,000 cal/mole are ≈1635° C, ~5 to 53 mole % Al_2O_3 at 1100°C, and ~3 (at ~920°C) and ~58 (at~600°C) mole % Al_2O_3. In light scattering studies on Al_2O_3 containing high SiO_2 glasses Nassau et al.[18] observed phase separation in the 6.44 mole %

Al_2O_3 composition but not in the 6.13 mole % composition. They also estimated the glass transition temperature for the 6.13 mole % glass to be ~780±30°C. Their values support the gap with the consolute temperature of ~1540°C. Based on experimental data MacDowell and Beall[5] proposed a miscibility gap between ~7 and 55 mole % Al_2O_3 at 1100°C and a consolute temperature of ~1650°C. Their data generally fits the shape and position of both calculated gaps except that their consolute temperature appears to be too high although they did indicate some uncertainty in estimating this temperature.

We also examined glass compositions inside the calculated miscibility gap by direct transmission electron microscopy to test if the expected immiscibility could be experimentally realized. Melts were homogenized at ≈1975°C for 2 hours in molybdenum crucibles and rapidly cooled in helium.

Sample preparation for electron microscopy by the commonly used ion-thinning methods was not possible due to the brittleness of the samples. Consequently, the as-prepared glass samples were crushed into a fine powder and gently blown onto a copper grid prior to insertion in the electron microscope. In some samples and edges of the fractured glass fragments were found thin enough for bean transmission in a high voltage (650 kv) electron microscope. A direct transmission electron micrograph of a 23 wt% Al_2O_3 (15 mole %) glass in the as-quenched condition is shown in Fig. 9. The morphology of the microstructure is typical of the type of phase separation observed in those regions of glass forming systems where nucleation and growth mechanisms are thought

to operate. The selected area diffraction pattern obtained from the phase separated droplets indicates an amorphous structure verifying the glass-in-glass immiscibility in this composition. Melts with greater than ≈25 mole % Al_2O_3 (≈35 wt% Al_2O_3) have a tendency to crystallize rapidly.[4] In view of this tendency, experimental verification of the phase boundaries of the calculated miscibility gaps in quenched glass samples is not likely to be obtained by electron microscopy methods. Furthermore, even the glasses prepared by ultra-fast quenching methods[19,20] either crystallize during the quench or at ≈1000°C during subsequent reheating.[5] Hence, the traditional methods of observing opalescence and clearing upon traversing the boundary of the miscibility gap may not be fruitful for varifying the calculated liquid-liquid metastable immiscibility in the present system above 1000°C. The experimental verification of the phase boundary in Al_2O_3-rich compositions can, however, be obtained by conducting crystallization studies on selected melts and inferring the temperature of the onset of phase separation from a quantitative analysis of the phases in the microstructure.

2. Immiscibility in Al_2O_3-rich Compositions

The thermodynamic data obtained by analyzing the Al_2O_3 liquidus curve (Table III, IV and Figs. 4,6) can similarly be assembled in Eq. 4 to obtain the values of the free energy of mixing as a function of composition. When such data are obtained using SiO_2 and Al_2O_3 as the components (Table III, Figs. 4,6), a miscibility gap is predicted with a consolute temperature of ≈1120°C at a critical composition of ~78 mole % Al_2O_3. This gap with its spinodal is included in Fig. 1. On the other hand if mullite (0.6 Al_2O_3 0.4 SiO_2) and Al_2O_3 are considered as

components, the upper consolute temperature of the calculated miscibility gap is greater than 2100°C at a critical composition of ~78 mole % Al_2O_3. The use of mullite as a component in this case is unrealistic since no immiscibility has been reported in this composition range at such a high temperature.

The large difference in the consolute temperature of the miscibility gaps calculated from the same Al_2O_3 liquidus curve underscores the necessity of choosing proper species for use in the solution model. While the location of a miscibility gap cannot be accurately predicted because of the limitations of the present model and inadequate data on mixing species in the melt, the positive deviations from ideality in all of the calculated thermodynamic data point to a very strong tendency toward liquid immiscibility in the Al_2O_3-rich compositions.

Prediction of immiscibility in Al_2O_3-rich glasses might appear to have limited utility. However, the widespread use of ultra fast quenching techniques such as a splat cooling and laser melting as research tools has made possible glass formation in some unusual compositions. Awareness of possible immiscibility regions could, therefore, be of some use. In the present study an attempt was made to characterize high alumina glasses (73, 80, and 90 wt% Al_2O_3) prepared by laser spin melting.* Although clear glasses could not be obtained in these compositions, considerable supercooling was observed. For example, the 73 wt% Al_2O_3 composition started to crystallize at an estimated temperature of ~700-

*Courtesy of R. A. Happe, North American Rockwell Corp., Downey, Calif.

800°C during the rapid quenching. This temperature is very close to the phase boundary of the spinodal curve for the miscibility gap in Al_2O_3-rich compositions calculated by the thermodynamic procedures described earlier. Such a phase separation may, perhaps, be the cause of spontaneous homogeneous crystallization commencing as the supercooled liquid separates rapidly in the unstable spinodal region.

Experimental realization of liquid immiscibility in Al_2O_3-rich glasses may be difficult in view of the problems of obtaining and retaining glasses. Furthermore, experimental verification of the phase boundaries of the miscibility gap in Al_2O_3-rich compositions will not be possible above ≈1000°C since any glasses formed crystallize rapidly[5] obliterating any evidence, were it there, for liquid immiscibility. The available experimental data suggests that the best hope for realizing possible immiscibility in Al_2O_3-rich compositions may lie in lengthy heat treatments of very rapidly cooled glasses in the temperature range ≈600-800°C.

IV. SUMMARY AND CONCLUSIONS

The regions of metastable immiscibility in the SiO_2-Al_2O_3 system have been calculated from the thermodynamic data derived from the phase diagram. A miscibility gap with a consolute temperature of ≈1540°C at an Al_2O_3 mole fraction of 0.36 has been calculated in the SiO_2-mullite pseudobinary system using a heat of fusion value of 27,000 cal/mole for mullite determined from the phase diagram shown in Fig. 1. Immiscibility in SiO_2-rich glasses has been experimentally verified by transmission electron microscopy studies.

The calculated thermodynamic data also suggest the possibility of immiscibility in Al_2O_3-rich compositions; problems in realizing such immiscibility are outlined. The thermodynamic data generated from the liquidus curves is of an approximate nature and uncertainties may arise due to the several assumptions inherent in the procedures used. However, in view of equally serious problems in obtaining direct experimental data for locating immiscibility, the present estimates may serve as a guide for workers studying phase separated glass structures and for those testing unusual glass forming compositions by exotic quenching techniques.

ACKNOWLEDGMENTS

Grateful acknowledgment is made to Leo Brewer, Richard J. Charles, Alexandra Navrotsky, and Alan W. Searcy for helpful discussions.

This study was supported by the U. S. Energy Research and Development Administration.

REFERENCES

1. R. J. Charles, "Immiscibility and Its Role in Glass Processing", Bull. Am. Ceram. Soc., 52, [9], 673-80 (1973).

2. F. Ya. Galakhov and S. F. Konovalova, "Liquidation Phenomena in the System Al_2O_3-SiO_2": I, Izv. Akad. Nauk SSSR, Ser. Khim, 1964 [8] 1373-77; "II", ibid, 1377-83.

3. D. Ganguli and P. Saha, "Macroliquation in the System Al_2O_3-SiO_2", Mater. Res. Bull., 2 [1], 25-36 (1967).

4. J. F. MacDowell and G. H. Beall, "Immiscibility and Crystallization in Al_2O_3-SiO_2 Glasses", J. Amer. Ceram. Soc. 52 [1], 17-25 (1969).

5. T. Takamori and R. Roy, "Rapid Crystallization of SiO_2-Al_2O_3 Glasses", J. Amer. Ceram. Soc., 56 [12] 639-644 (1973).

6. J. Chipman, "Activities in Liquid Metallic Solutions", Disc. of the Faraday Society, No. 4, pp 23-49 (1948).

7. T. Forland, "Thermodynamic Properties of Fused-Salt Systems", in "Fused Salts", pp 63-164 edited by B. R. Sundheim, McGraw Hill Book Co., (1964).

8. M. Rey, "The Thermodynamic Acitvity of Silica and of Oxides in Silicate Melts", ibid, pp 257-265.

9. R. J. Charles, "Activities in Li_2O- Na_2O - and K_2O-SiO_2 Solutions", J. Amer. Ceram. Soc. 50, [12] 631-641 (1967).

10. R. J. Charles, "Metastable Immiscibility in the B_2O_3-SiO_2 System", ibid, 51 [1] 16-20, (1968).

11. W. Haller, D. H. Blackburn and J. H. Simmons, "Miscibility Gaps in Alkali Silicate Binaries - Data and Thermodynamic Interpretation", J. Amer. Ceram. Soc., 57 [3] 120-126 (1974).

12. I. A. Aksay and J. A. Pask, "Stable and Metastable Equilibria in the SiO_2-Al_2O_3 System", J. Am. Ceram. Soc., 58 [11-12] 507 (1975).

13. M. A. Moseman and K. S. Pitzer, "Thermodynamic Properties of the Crystalline Forms of Silica", J. Am. Chem. Soc. 63, 2348 (1961).

14. E. E. Shpilrain, D. N. Kagan and L. S. Barkhatov, "Thermodynamic Properties of the Condensed Phase of Alumina Near the Melting Point", High Temperatures-High Pressures, 4, [6] 605-609 (1972).

15. P. C. Hess, "PbO-SiO_2 Melts: Thermodynamics of Mixing", Geochim. et. Cosmo Chim. Acta, 39, 671 (1975).

16. J. H. Hildebrand and R. L. Scott, Solubility of Nonelectrolytes, p 35, Dover Publications Inc., N. Y. 1964 (3rd Ed.).

17. R. Rossin, J. Bersan and G. Urbain, "Viscosity of Fused Silica and Glass Belonging to the SiO_2-Al_2O_3 System", C. R. Acad. Sci. 258 [2], 562-64 (1964).

18. K. Nassau, J. W. Shiever and J. T. Krause, "Preparation and Properties of Fused Silica Containing Alumina", J. Am. Ceram. Soc. 58 [9-10] 461 (1975).

19. L. E. Topol, D. H. Hengstenberg, M. Blander, R. A. Happe, N. L. Richardson and L. S. Nelson, "Formation of New Oxide Glasses by Laser Spin Melting and Free Fall Coolins, J. Non. Cryst. Solids, 12, 377-390 (1973).

20. R. Krepski, K. Swyler, H. R. Carleton and H. Herman, "Liquid Quenching of Laser Melted Oxides", J. Mat. Sci. 10 [8] 1452-1454 (1975).

21. S. H. Risbud and J. A. Pask, "Crystallization of SiO_2-Al_2O_3 Melts", in preparation.

Table I. Thermodynamic Data From the Silica Liquidus.

Mole Fraction of Mullite (Liquidus Compositions)	Liquidus Temp. (°K)	Activity of SiO_2	$Log_{10}\gamma^{\ell}_{SiO_2}$	Partial Molal Heat of Solution, cal/mole
.0167	1973	0.994	+0.0047	42.4
.043	1927	0.983	+0.0116	102
.067	1903	0.977	+0.020	174
0.086	1860	0.966	+0.024	204

Table II. Thermodynamic Data from the Mullite* Liquidus.

Mole Fraction Mullite (Liquidus) Compositions)	Liquidus Temp.(°K)	$\text{Log}_{10}\gamma^{\ell}_{\text{Mullite}}$	Partial Molal Heat of Solution, cal/mole
0.086	1860	0.633	5387
0.129	1953	0.609	5441
0.172	1998	0.552	5046
0.215	2013	0.477	4393
0.258	2025	0.415	3845
0.344	2048	0.323	3026
0.430	2059	0.241	2270
0.515	2079	0.191	1817
0.601	2090	0.139	1329
0.687	2101	0.095	913
0.773	2115	0.063	610
0.859	2122	.026	252

*Heat of fusion ≃ 27,000 cal/mole.

Table III. Thermodynamic Data from Al_2O_3 Liquidus with SiO_2 and Al_2O_3 as Components.

Mole Fraction Al_2O_3 (Liquidus Composition	Liquidus Temp. (°K)	$Log_{10}\gamma^{\ell}_{Al_2O_3}$	Partial Molal Heat of Solution, cal/mole
0.40	2105	0.14441	1390.7
0.45	2148	0.14779	1452.4
0.50	2195	0.15895	1596.2
0.55	2205	0.12933	1304.7
0.60	2226	0.11586	1179.9
0.65	2243	0.10042	1030.5
0.70	2254	0.08057	830.8
0.75	2266	0.06390	662.4
0.80	2280	0.05118	533.9
0.85	2288	0.03351	350.8
0.90	2301	0.02261	238.0
0.95	2310	0.00866	91.5
1.00	2323	0.0000	≈0

Table IV. Thermodynamic Data from Al_2O_3 Liquidus with Mullite (0.6 Al_2O_3 0.4 SiO_2) and Al_2O_3 as Components.

Mole Fraction Al_2O_3 (Liquidus Composition)	Liquidus Temp. (°K)	$Log_{10}\gamma^{\ell}_{Al_2O_3}$	Partial Molal Heat of Solution, cal/mole
0.010	2226	1.894	19394
0.125	2243	0.816	8420
0.188	2253	0.650	6737
0.250	2257	0.528	5481
0.312	2261	0.439	4566
0.375	2266	0.365	3805
0.438	2273	0.305	3189
0.500	2280	0.255	2675
0.625	2288	0.167	1758
0.750	2301	0.102	1080
0.812	2306	0.071	753
0.938	2316	0.021	224
1.000	2323	0.000	0

Table V. Effect of Heat of Fusion of Mullite on Calculated Liquid Miscibility Gaps for Metastable SiO_2-3:2 Mullite (0.58 Al_2O_3) System.

Heat of Fusion of Mullite (cal/mole)	Upper Consolute Temp. (±10°C)	Critical Composition, mole% Al_2O_3
16,000	1635	36,0
27,000	1540	35.5
36,000	1380	35.0
45,000	1230	34.5
53,000	1090	34.0
72,000	725	34.0

FIGURES

1. Calculated miscibility gaps superimposed on stable and metastable phase equilibra diagrams for the SiO_2-Al_2O_3 system (Ref. 12).
2. Activity coefficients of mullite for the metastable SiO_2-3:2 mullite (0.58 Al_2O_3·42 SiO_2) system using heat of fusion for mullite of 27,000 cal/mole.
3. Activity coefficients of SiO_2 for the metastable SiO_2-3:2 mullite (0.58 Al_2O_3·0.42 SiO_2) system using heat of fusion for mullite of 27,000 cal/mole.
4. Activity coefficients of Al_2O_3 calculated from the Al_2O_3 liquidus over the range of 40 to 100 mole% Al_2O_3 using SiO_2 and Al_2O_3 as immiscibility species.
5. Activities of Al_2O_3 at several subliquidus temperatures over the range of 40 to 100 mole% Al_2O_3.
6. Activity coefficients of SiO_2 from the Al_2O_3 liquidus over the range of 40 to 100 mole% Al_2O_3.
7. The α- function for the stable SiO_2-Al_2O_3 phase equilibrium diagram.
8. Isothermal free energy of mixing for several temperatures for the metastable SiO_2-3:2 mullite (0.58 Al_2O_3) diagram using a heat of fusion for mullite of 27,000 cal/mole.
9. Direct transmission electron micrograph of 15 mole% (23 wt%) Al_2O_3 glass showing phase separated glassy droplets (≃400 Å) in a glass matrix. Inset shows a selected area diffraction pattern from a droplet showing predominantly amorphous structure.

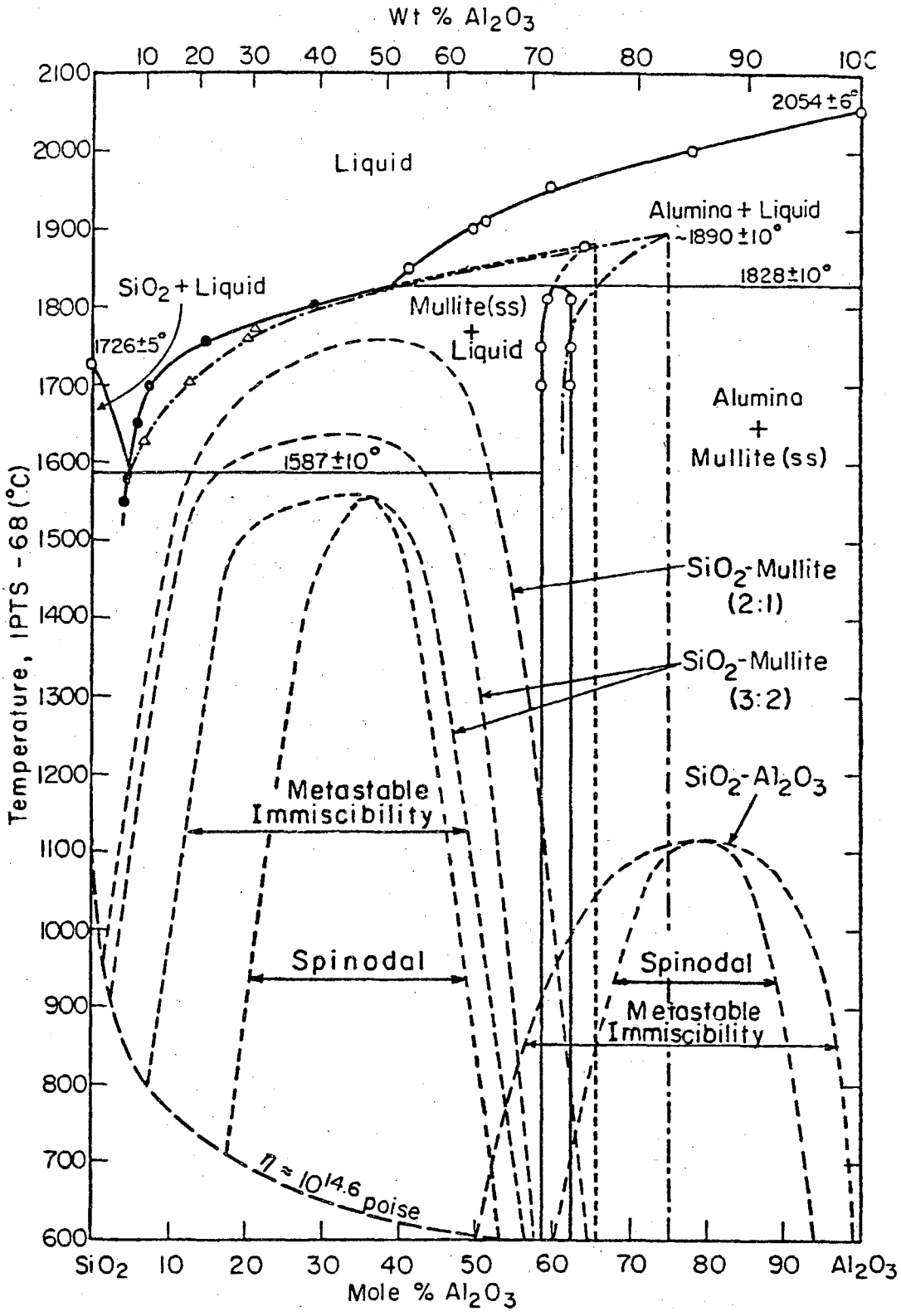

XBL 766-7008B
Fig. 1

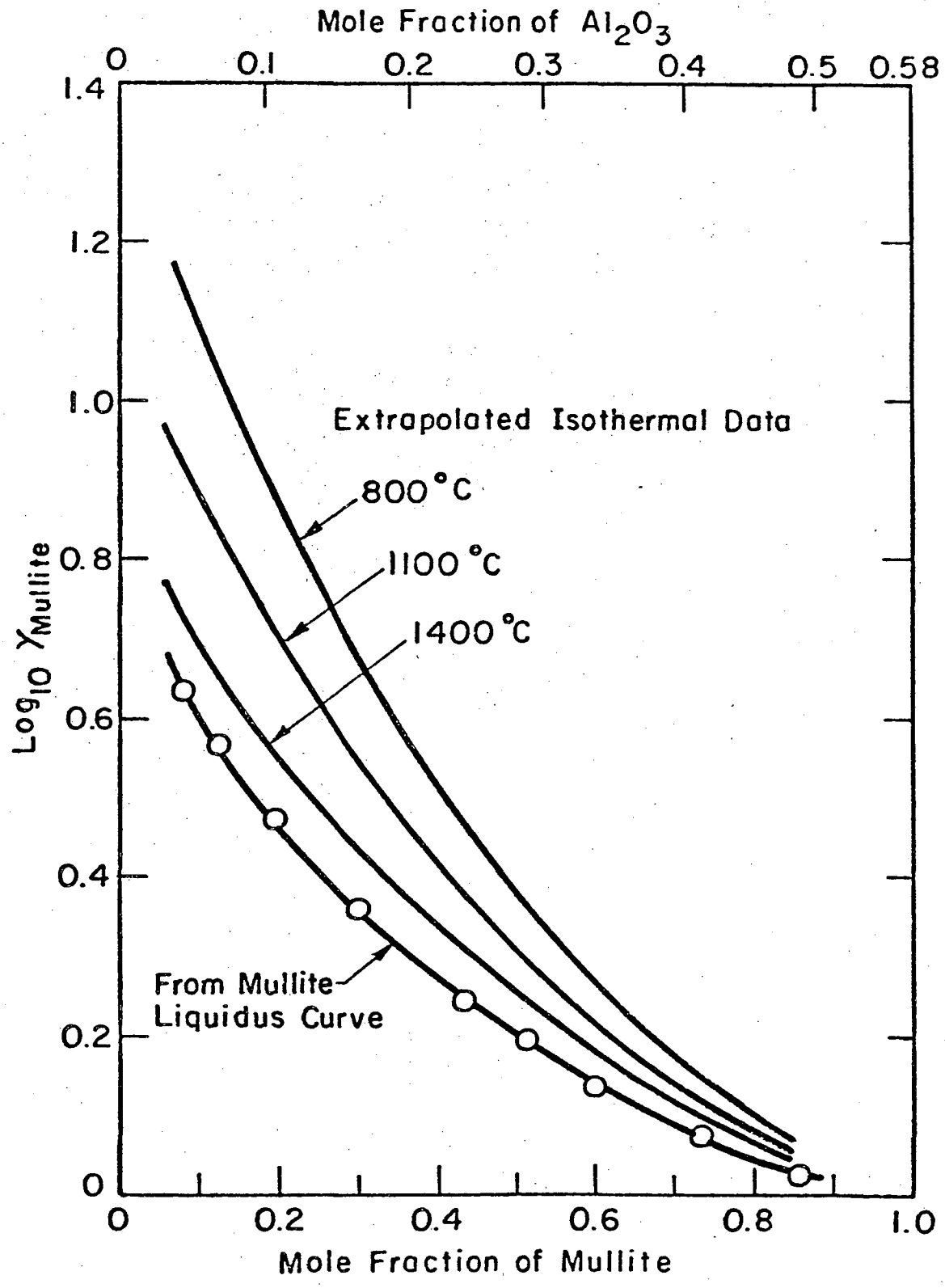

XBL 768-7334

Fig. 2

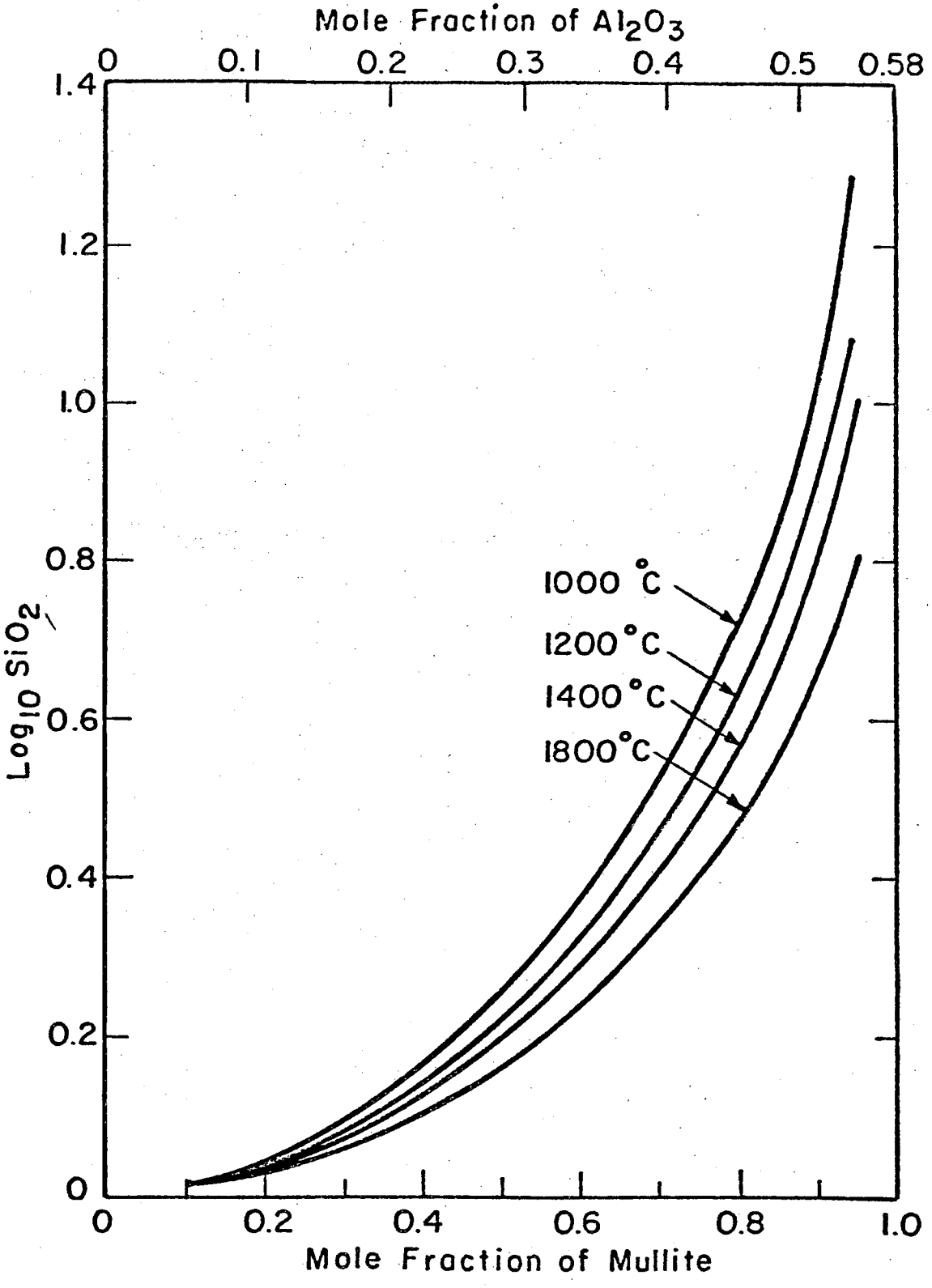

XBL 768-7336

Fig. 3

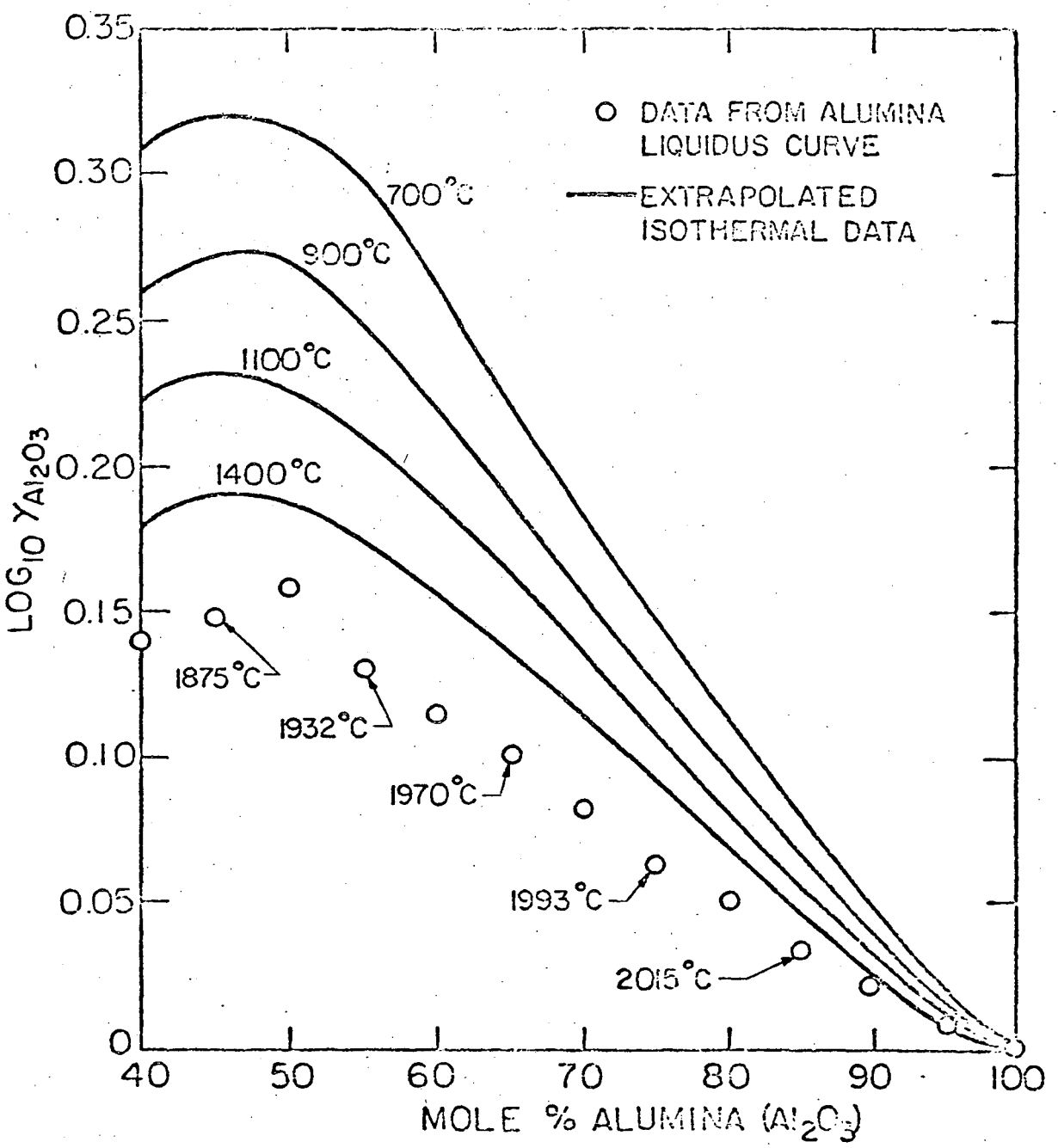

XBL757-6822

Fig. 4

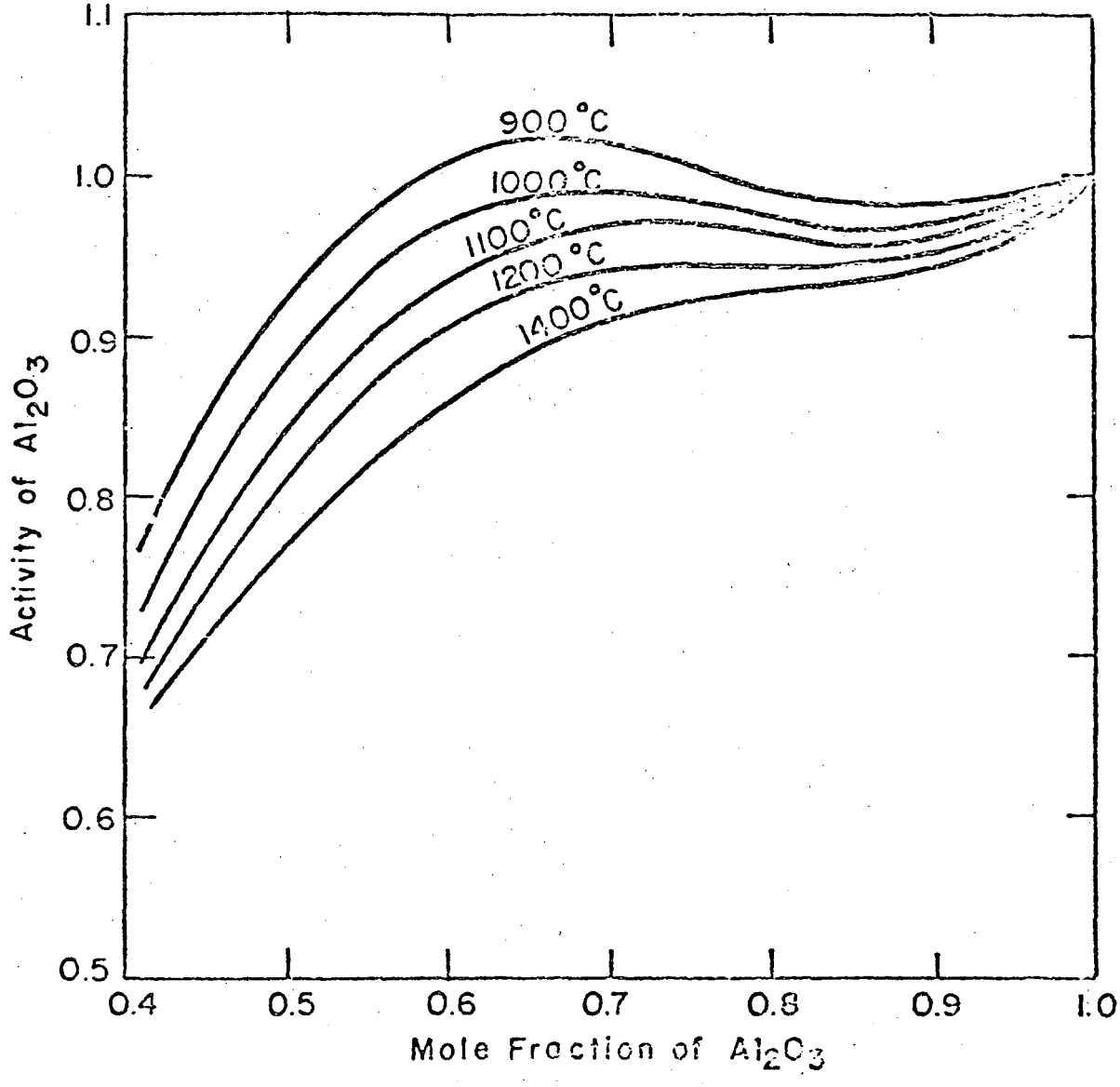

XBL765-6838
Fig. 5

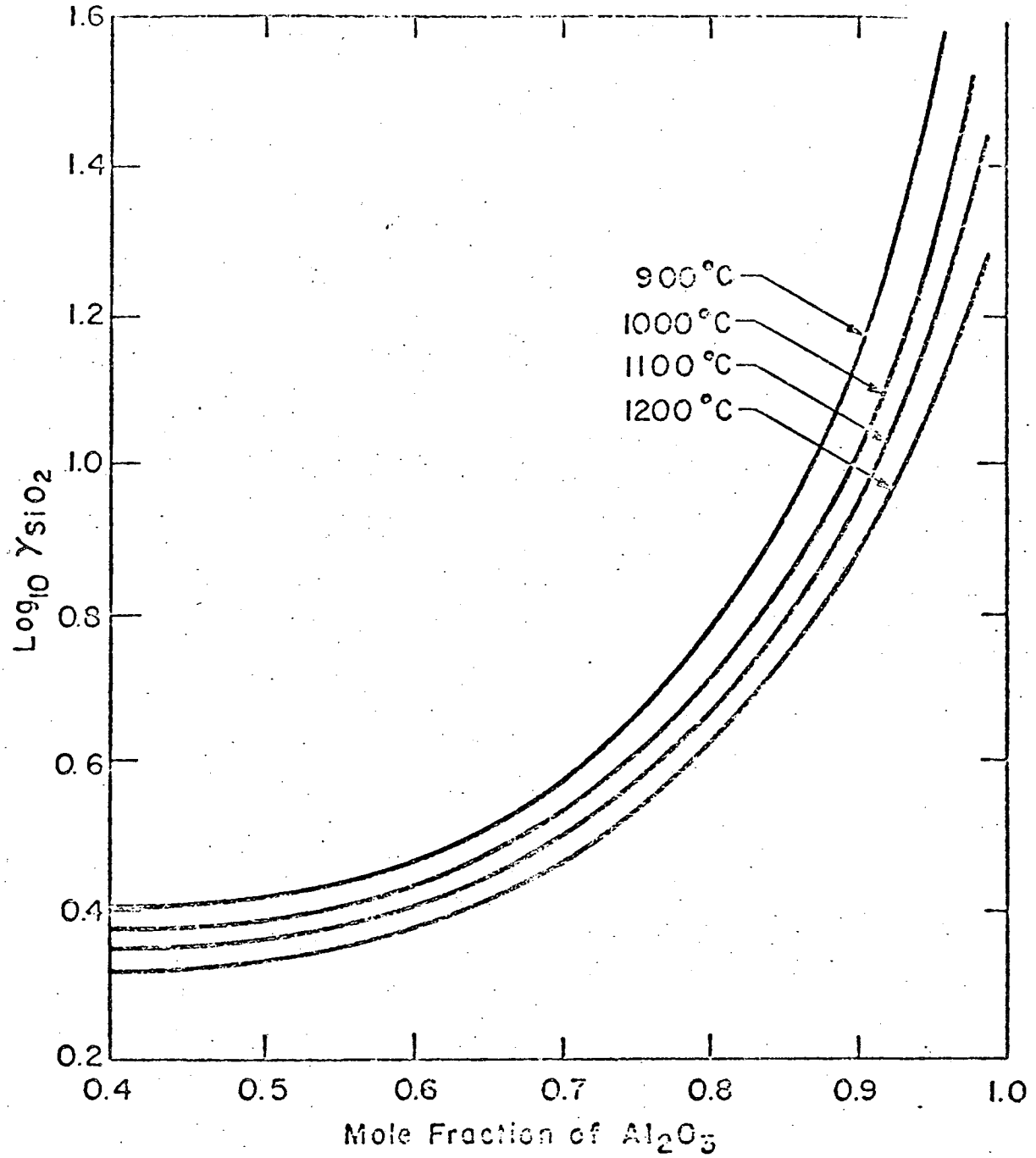

XBL765-3883

Fig. 6

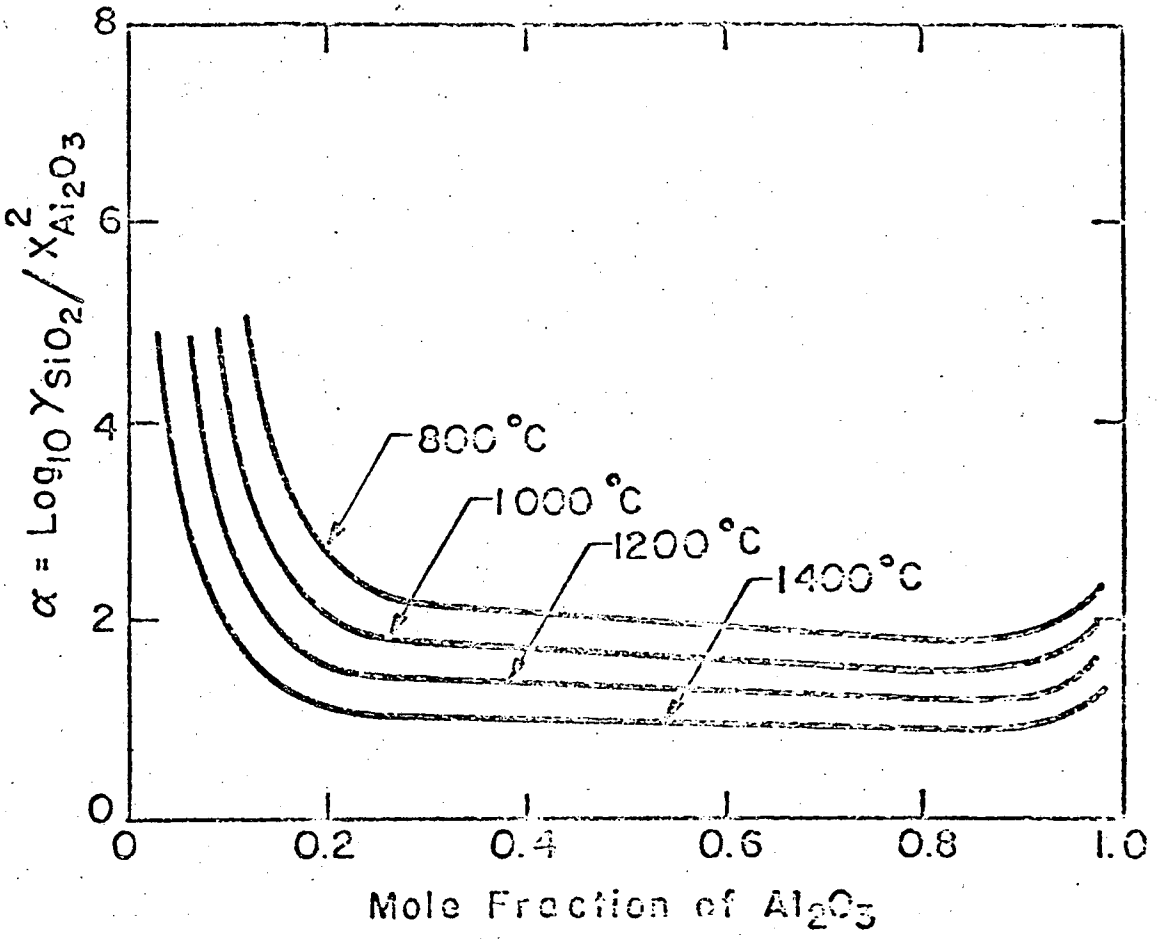

XBL765-6887

Fig. 7

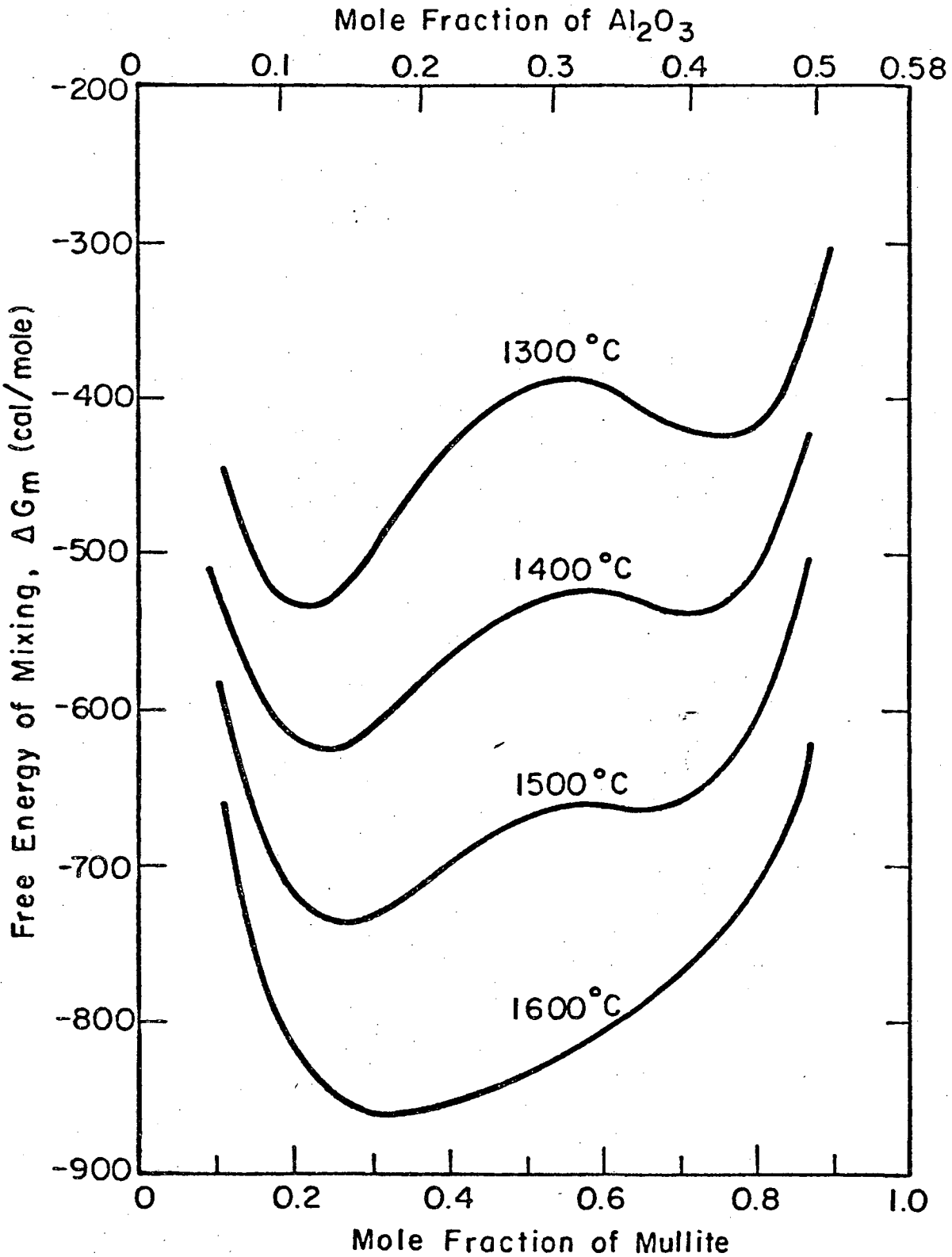

XBL 768-7335

Fig. 8

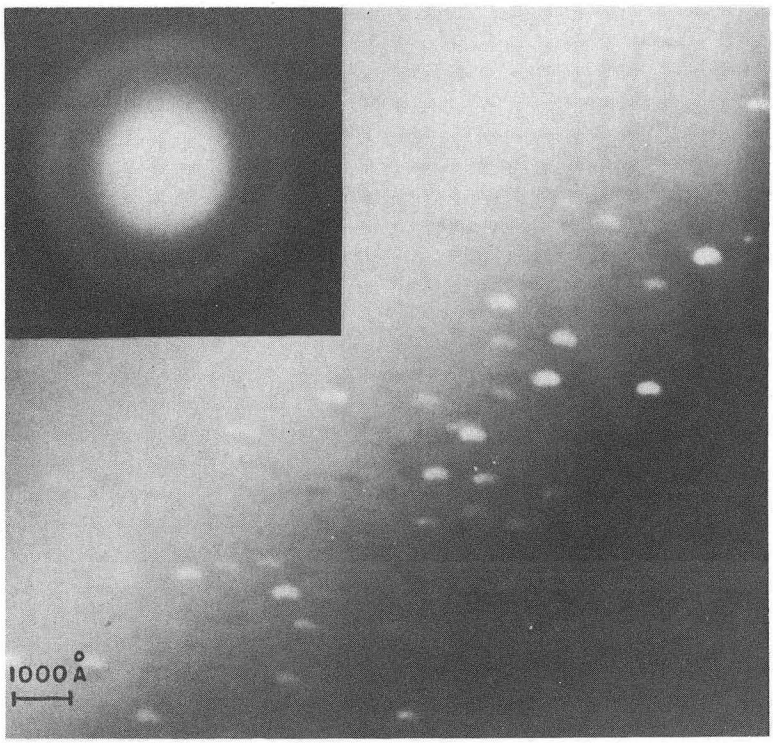

XBB766-4825A
Fig. 9

This report was done with support from the United States Energy Research and Development Administration. Any conclusions or opinions expressed in this report represent solely those of the author(s) and not necessarily those of The Regents of the University of California, the Lawrence Berkeley Laboratory or the United States Energy Research and Development Administration.

TECHNICAL INFORMATION DIVISION
LAWRENCE BERKELEY LABORATORY
UNIVERSITY OF CALIFORNIA
BERKELEY, CALIFORNIA 94720